76295

Impact Melt Breccia
260.7 g, 10 x 6 x 3.5 cm

INTRODUCTION

Sample 76295 was chipped from Block I of the big boulder at Station 6 (Wolfe and others, 1981, Heiken et al., 1973). It is a non-vesicular, crystalline matrix breccia with a blue-grey color (similar to 76275). Light and dark clasts have a distinct outline with the matrix (Fig. 1), and the fine grain size of the matrix of this sample and that of 76275 form an important argument of the thermal model of Simonds (1975) and Onorato et al. (1976) for the genesis of impact melt breccias.

PETROGRAPHY

Sample 76295 is a banded, clast-bearing, nonvesicular, blue-grey breccia with aphanitic matrix. The modal mineralogy of 76295 is about 50% plagioclase, 40% low-calcium pyroxene, with minor amounts of augite, olivine, ilmenite, armalcolite, and metallic iron. The texture of the fine grain matrix of 76295 is subophitic (Simonds et al., 1974). The matrix consists predominantly of low-calcium pyroxene ($Wo_4En_{60-73}Fs_{19-26}$), minor augite ($Wo_{30-40}En_{44-57}Fs_{12-15}$), Olivine ($Fo_{70-76}$), and feldspar ($An_{81-97}$). The grain size of matrix feldspar is <15 µm, pyroxene 10-25 µm (Fig. 2).

Banded areas of aphanitic tan matrix are included in the aphanitic blue-grey matrix (Fig. 3). There are only minor differences between the mineralogy of the tan areas and that of the blue-grey matrix (Fig. 4). There appears to be significantly more olivine in the blue-grey portions and more augite in the tan

Figure 1: Freshly broken surface of impact melt breccia 76295. Scale is 1 cm. S72-56409.

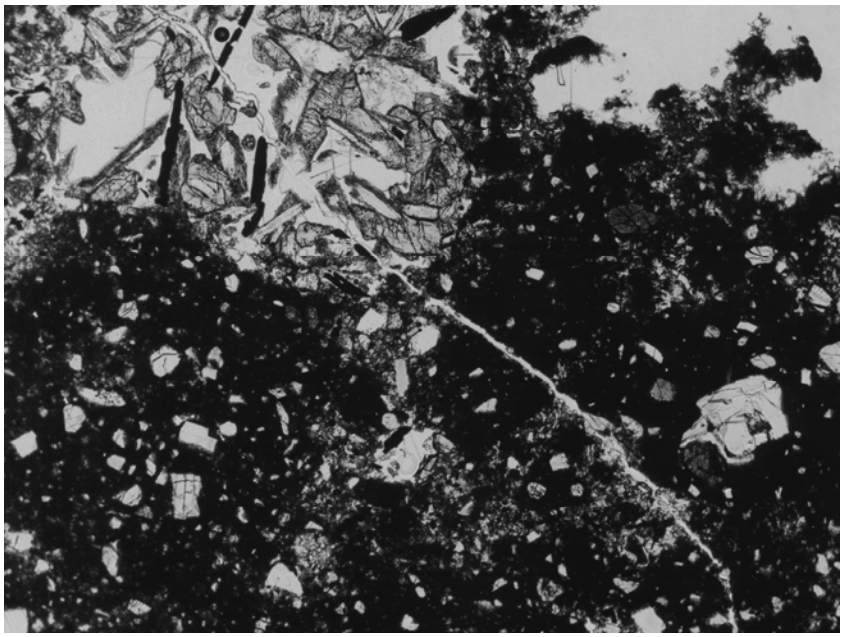

Figure 2: Photomicrograph of 76295,85, showing fine grain aphanitic matrix and vesicular basalt clast. Field of view is 4 x 5 mm.

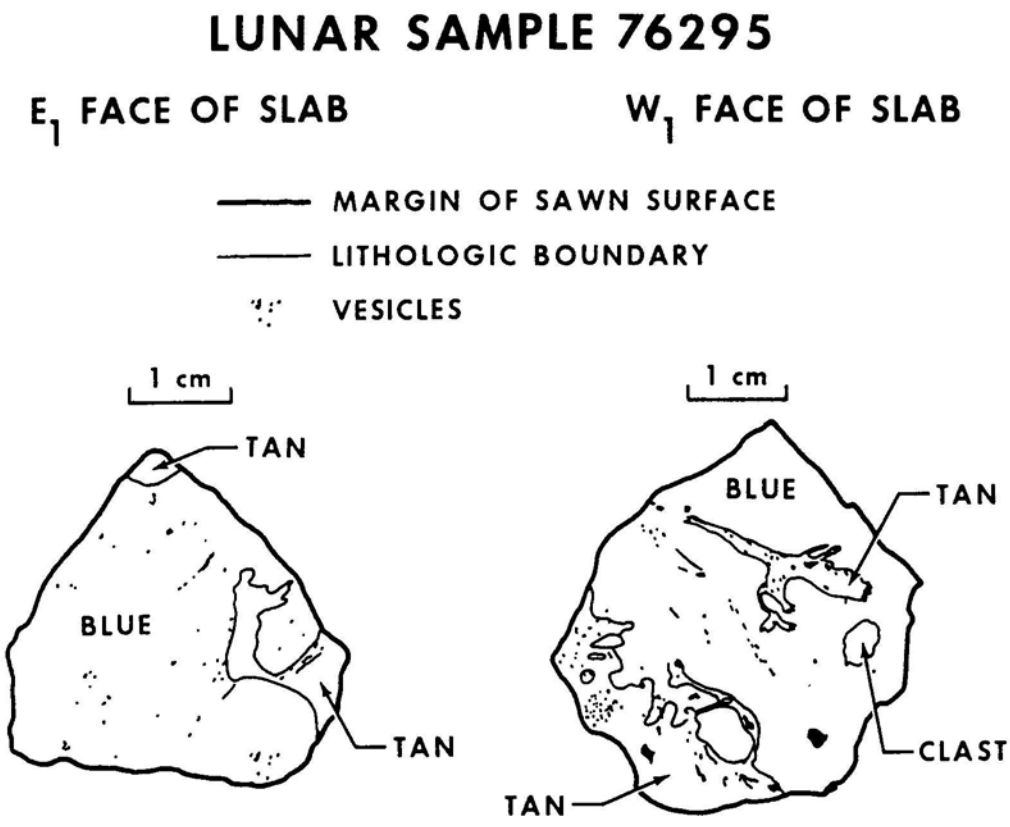

Figure 3: Maps of two slab surfaces through sample 76295.

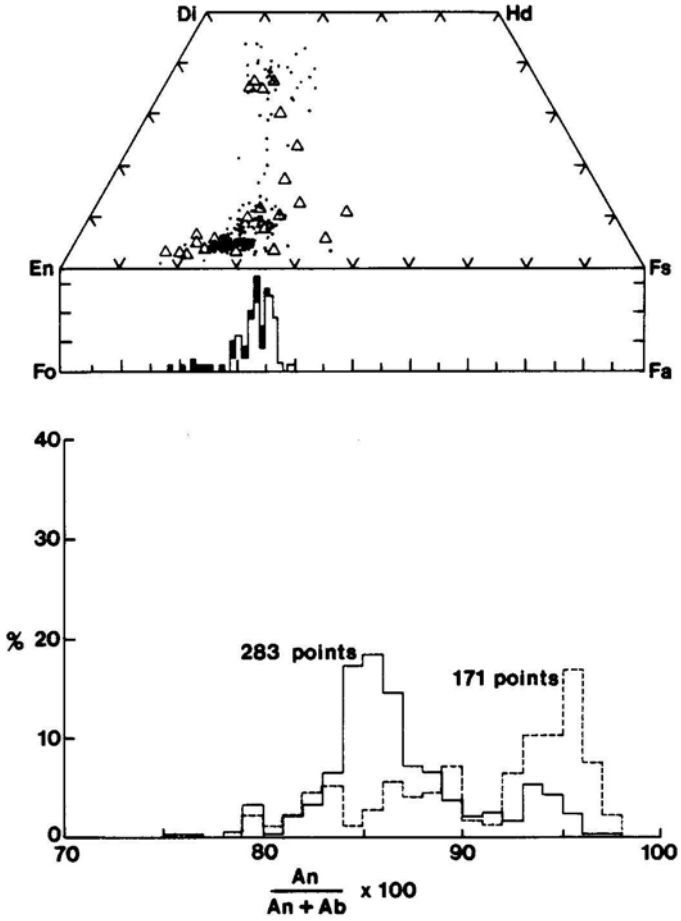

Figure 4: Mineral composition of blue-grey matrix and tan-grey clast veins in 76295. From Phinney (1981).

areas, but this is not well documented. Rare rounded clasts (50 pm) of pink spinel are found in the blue-grey subophitic matrix (Simonds, 1975).

Norman et al. (1993) have compared the composition of minerals in LKFM clasts in 76295 with minerals in similar clasts in 76315 (Fig. 5). They conclude that the clast population in 76295 is dominated by "Mg-suite norites, troctolites and gabbronorites." Minor-element abundances in both olivine and pyroxene are unlike those found in lunar rocks of the ferroan anorthosite suite.

Misra et al. (1976) have studied the complex metallic nickel-iron particles included in 76295.

WHOLE-ROCK CHEMISTRY

The matrix of 76295 is homogeneous and apparently similar to that of the other samples of this boulder (Fig. 6). Unpublished chemical data are :reported in Phinney (1981). There is no difference between the REF composition of the tan matrix and that of the blue-grey matrix (Table 1). Higuchi and Morgan (1975) find that the trace siderophile element composition of the matrix of 76295 is within the tight grouping of the Station 6 Boulder (meteorite group 2) on the Ir-Au-Re compositional diagram, but that the Ir-Au-Re ratios of the 76295 clasts are distinctly different (Fig. 7). The 76295 matrix has a higher abundance of these meteoritic elements than the matrix for 76015 and 76215 (Table 2). Some data for 76295 are also given in Simonds and Warner (1981).

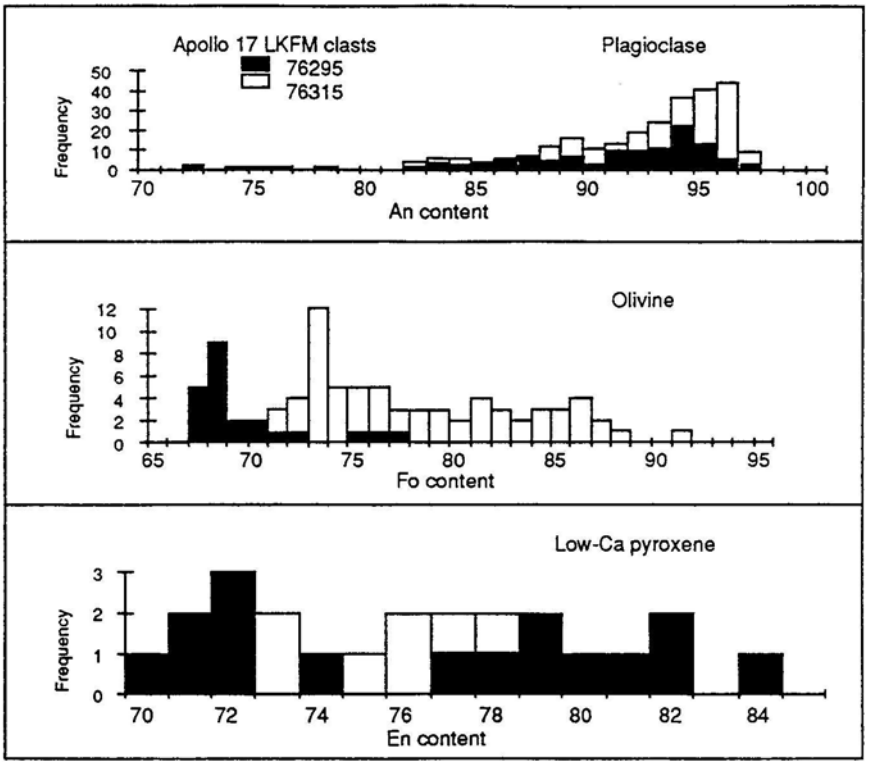

Figure 5: Histograms of plagioclase, olivine, and pyroxene compositions of clasts in 76295 and 76315. From Norman et al. (1993).

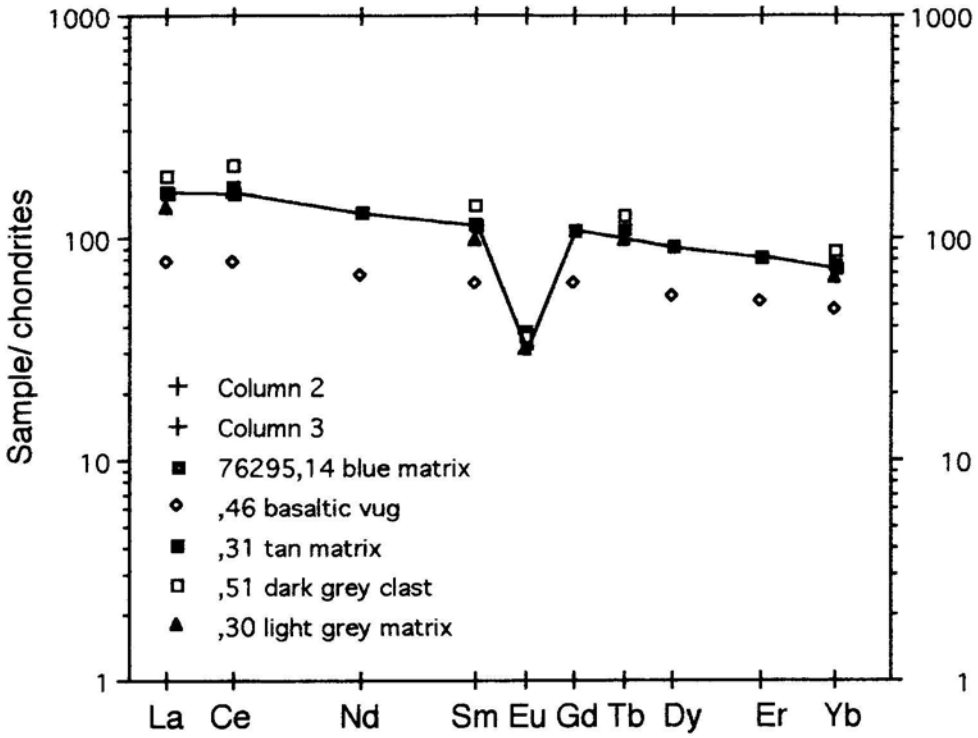

Figure 6: Normalized rare earth element diagram for matrices and clasts in breccia 76295. The blue-grey and tan matrices have the same exact composition. The dark grey clast has higher REE and the basalt is lower. The basalt is not like a mare basalt.

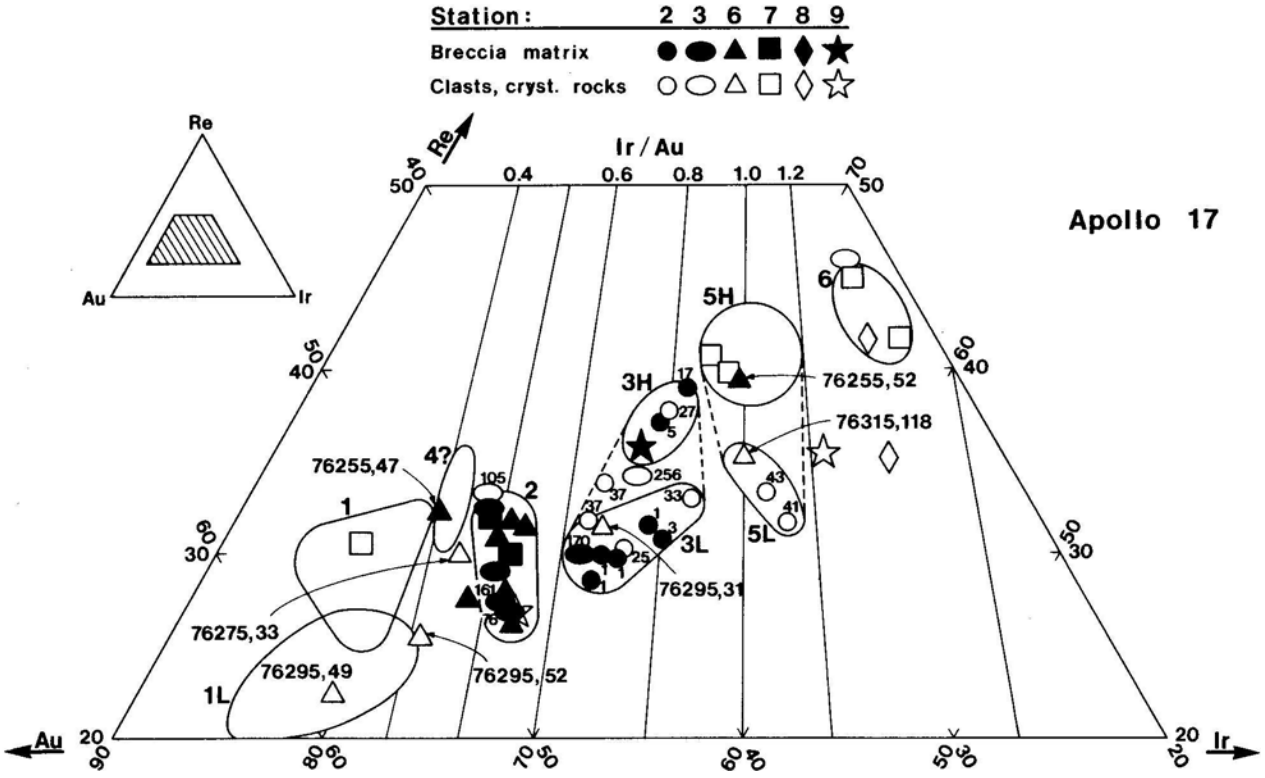

Figure 7: Ir-Au-Re diagram from Higuchi and Morgan (1975), showing that the 76295 clasts are slightly different from the breccia matrix (group 2).

SIGNIFICANT CLASTS

The dark grey and light grey aphanitic clasts analyzed by Phinney (1981) are, respectively, subophitic and poikilitic melt rocks quite similar to the fragments that form the matrix of the boulder. They have slightly higher KREEP contents than the matrix (Fig. 6).

Four small vuggy basalt clasts (similar to the large basaltic vug in 76015) occur in 76295. Because of their high porosity, these "clasts" appear to be vu fillings. Their texture is that 4 an intersertal basalt, but with pore spaces in place of mesostasis (Fig. 2). Plagioclase occurs as subhedral grains up to 300 gm long with inclusions of pyroxene, K-feldspar, opaques, and a silica phase concentrated at the rims (Phinney, 1981). Fig. 8 gives the mineral compositions of a porous basalt clast (from Simonds, 1975). The composition of the porous basaltic clast (see Table 1) is quite exotic, with preferential enrichment in the volatile elements such as Rb relative to U (Simonds, 1975).

Simonds (1975) also studied the mineral composition of a "troctolite" clast in 76295 (Fig. 9).

RADIOGENIC ISOTOPES

Cadogan and Turner (1976) determined the crystallization age of two samples of 76295 by the ^{39}Ar-$^{40}Ar_r$ plateau technique. The tan matrix yielded an intermediate temperature plateau age of 3.95 ± 0.04 b.y., and the blue-grey matrix yielded one of 3.96 ± 0.04 b.y. Both exhibited appreciable high-temperature decreases in ^{40}Ar over the last 30% release (Fig. 10).

Unpublished U-Th-Pb data by Leon Silver were reported in Phinney (1981).

COSMOGENIC RADIOISOTOPES AND EXPOSURE AGES

Some of the Apollo 17 samples (including 76295) provided a unique opportunity to study the energy spectrum (and potential angular anisotropy) of the incident proton flux from the August 1972 solar flare (Rancitelli et al., 1974; Keith et al., 1974).

Bogard et al. (1974; see unpublished data in Phinney, 1981) have deter-mined the noble gas abundances in 76295.

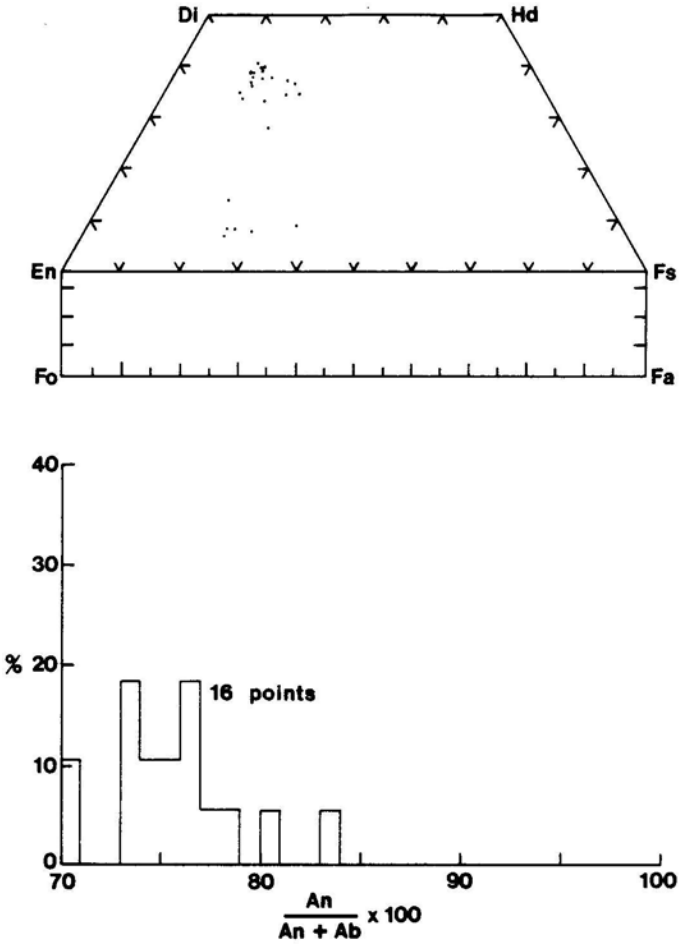

Figure 8. Microprobe analyses of minerals in a porous basaltic clast in 76295. From Simonds (1975).

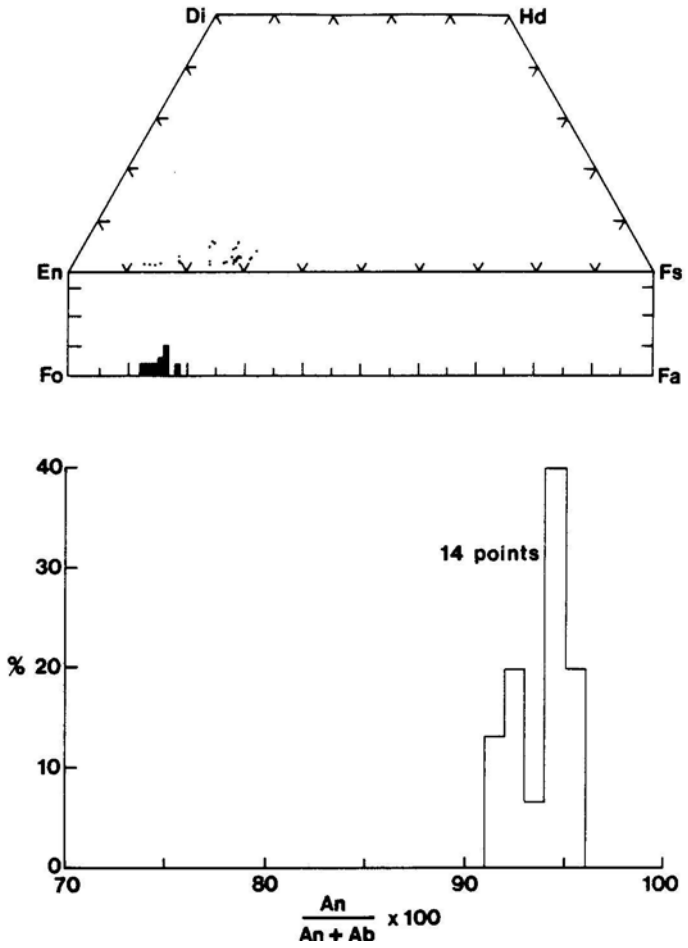

Figure 9: Microprobe analyses of minerals in a "troctolite" class in breccia 76295. From Phinney (1981).

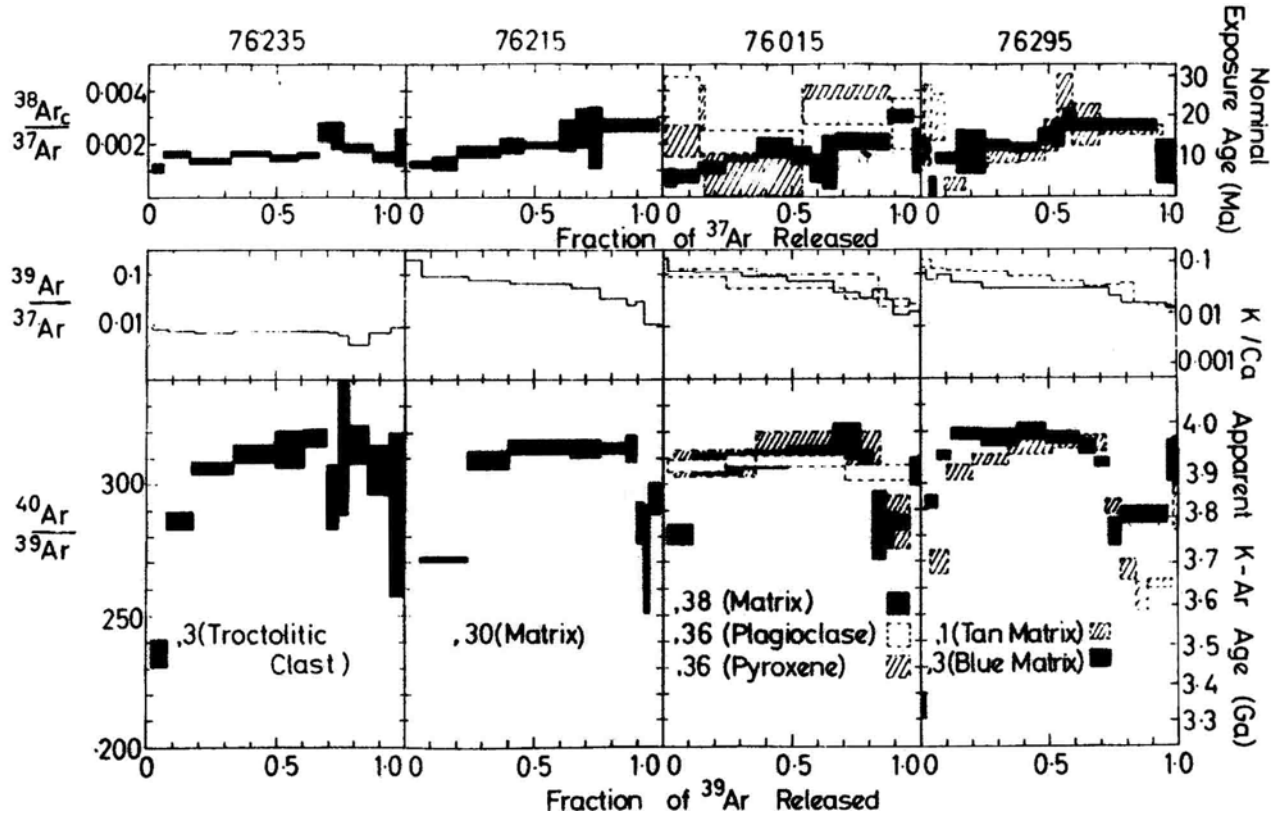

Figure 10: Ar-Ar release diagram for 76295 matrix:. By Cadogan and Turner (1976).

MAGNETIC STUDIES

Gose et al. (1978) have carefully studied the remanent magnetization of 26 subsamples from the Station 6 Boulder. The direction of magnetization after alternating field demagnetization of breccia sample 76295 was found to be scattered for this clast-rich sample. Gose et al. propose that the large scatter of magnetization direction of 76295 implies the predominance of pre-impact magnetization in this sample. Brecher (1976) is convinced that alignment of magnetism follows the direction of foliation and is caused by "textural remanent magnetization."

PROCESSING

A slab and a column were cut from this rock (see lithology maps and diagrams in Phinney, 1981).

Table 1: Whole-rock chemistry of 76295.
a) Simonds (1975); b) Wiesmann and Hubbard (1975); c) Phinney (1981)

Split Technique	,14 (a, b) IDMS blue matrix	,46 (b, c) fused bead basaltic vug	,31 ,35 (c) INAA tan matrix	,51 (c) INAA dark grey clast	,30 (c) INAA light grey clast
SiO_2 (wt%)	47.03	48.11	47.55	46.89	47.04
TiO_2	1.39	1.80	1.64	1.50	1.36
Al_2O_3	18.25	16.95	17.67	18.67	18.98
Cr_2O_3	–	0.17	0.17	0.17	0.16
FeO	9.09	9.17	9.05	8.79	8.44
MnO	–				
MgO	10.78	9.72	9.78	9.66	9.64
CaO	11.54	11.22	11.49	11.69	11.95
Na_2O	0.76	0.7	0.74	0.71	0.66
K_2O	0.26	0.6	0.29	0.23	0.28
P_2O_5	0.32				
S	0.06				
Nb (ppm)					
Zr	541	232			
Hf	–	–	13.2	16.3	12.4
Ta			1.9	2.4	1.7
U	1.83	0.66			
Th	6.12	2.01	5.6	7.6	5.2
Sr	–	191			
Rb	5.43	20.47			
Li	19.4	20.5			
Ba	376	334			
Ni			160	220	170
Co			19.9	28	23
Sc			17.8	18.2	16.7
La	37.8	18.2	37.5	44.2	31.8
Ce	95.7	46.6	102	127	95.8
Nd	60.0	31.1			
Sm	16.9	9.22	17	20.4	14.3
Eu	1.91	2.08	2.11	2.01	1.77
Gd	21.3	12.4			
Tb			3.91	4.56	3.56
Dy	22.3	13.3			
Er	13.2	8.06			
Yb	12.0	7.6	12.2	14.1	10.8
Lu	–	1.07	1.71	1.95	1.49

Table 2: Trace element data for 76295 matrix and clast. Concentrations in ppb.
From Higuchi and Morgan (1975).

	Sample 76295,31 clast	Sample 76295,34 matrix	Sample 76295,37 matrix	Sample 76295,49 basalt	Sample 76295,52 clast
Ir	5.98	6.1	7.88	3.18	5.42
Os					
Re	0.48	0.486	0.566	0.267	0.456
Au	2.65	3.43	4.36	2.91	3.93
Pd					
Ni (ppm)	179	218	250	146	203
Sb	1.03	1.68	393	1.84	2.11
Ge	198	374	316	321	423
Se	75	132	103	235	68
Te	2.4	4.62	4.9	5.81	1.9
Ag	0.87	5.09	4.55	1.03	1.2
Br	23.5	27.9	78.7	30.5	37.5
In					
Bi	0.46	0.8	0.97	0.4	0.56
Zn (ppm)	2.3	2.5	27.1	2.2	2.6
Cd	1.88	1	6.56	1.13	1.28
Tl	0.44	0.64	1.41	0.99	0.33
Rb (ppm)	3.31	4.22	9.2	12.5	1.75
Cs	192	297	151	649	110
U	1620	1320	1910	760	1940